LuSci, a lunar scintillometer to study ground layer turbulence

Jayadev Rajagopal[a], A. Tokovinin[a], E. Bustos[a] and J. Sebag[b]

[a]NOAO/CTIO, Casilla 603, La Serena, Chile;
[b]NOAO, 950 N.Cherry Ave., Tucson, AZ 85719, USA.

ABSTRACT

We present a new lunar scintillometer, LuSci. A simple and accurate way to determine the Ground Layer (GL) turbulence profile is through measuring lunar and solar scintillation. The contribution of the first 10-100 m to the total seeing is usually significant. Measuring the seeing in this GL is important to evaluate sites, especially to set the height of future domes and to translate existing seeing data to higher domes. This holds in particular to Antarctic sites where the GL seeing is dominant, with obvious implications for AO and interferometry. We develop robust methods for turbulence profile restoration from LuSci data, incorporating the effect of lunar phases. We present restored profiles from initial campaigns. We also extract a simple model for the wind profile from the rich information present in the scintillation spectrum.

Keywords: Seeing, Lunar scintillation, Atmospheric Turbulence

1. INTRODUCTION

Ground Layer (GL) turbulence in the first few hundred meters of the atmosphere makes a sizeable contribution to the overall seeing, sometimes up to 70 %.[1] Measuring the seeing profile close to the ground is important for various reasons:

1 Most seeing monitors for site surveys are placed a few meters above the ground, whereas the height of future telescope domes are likely to be few tens of meters. Knowledge of the seeing profle at such heights could enable the placement of these domes above the bulk of the seeing, on the average. This is especially true in sites like the Antarctic where almost all the seeing originates in the GL.

2 Current and future techniques to achieve high resolution like Ground Layer AO and Interferometry will benefit a great deal from knowledge of the behavior of seeing in the lower atmosphere which affects them critically.

1.1 Scintillation

The theory of stellar scintillation ("twinkling") is fairly well developed.[2] Turbulence in the atmosphere introduces temperature, pressure and density fluctuations, inducing refractive index variations which imprint themselves on the propagating wavefront as phase fluctuations. The intensity variation or scintillation at the ground level are a result of the focussing and defocussing effects of these fluctuations. Following Tatarski (1961, Ref. 3), the Structure Function $D_n(r)$ or the mean squared difference in refractive index over neighboring points in the horizontal plane provides fairly complete information on the refractive index variations. From Roddier (1981, Ref. 2), the seeing parameter, r_0, is related to the integral of the structure function constant $C_n^2(h)$ through

$$r_0^{-5/3} = 16.6\lambda^{-2} sec(\gamma) \int_0^\infty C_n^2(h)\mathrm{d}h \tag{1}$$

and the scintillation index or mean variance σ_I^2 of fluctuations for finite apertures on a point source is

$$\sigma_I^2 \propto \lambda^0 \int_0^\infty h^2 C_n^2(h)\mathrm{d}h. \tag{2}$$

For an extended source like the Moon, the scintillation index is similar to Eqn. 2 and is wavelength independent, but with a different altitude weighting for the integral. The two relations show that both scintillations and the seeing trace their origins to the very same turbulence, hence the notion of using the former to gauge the seeing profile.

E-mail: jrajagopal@ctio.noao.edu

1.2 Lunar Scintillation

In the case of the Moon (or the Sun), the scintillations are averaged over: 1) The section of the beam, $\sim \theta z$, where θ is the angular diameter of the Moon and z = $hsec(\gamma)$ is the distance to the turbulence layer at height h and zenith angle γ and 2) the diameter of the receiver aperture, d. The combination of these two is roughly equivalent to an effective diameter $d_e = \sqrt{\theta z^2 + d^2}$, and the averaging dampens the response to large heights. The sensitivity to lower layers ($z \ll d/\theta$) increases roughly as z^2, reaching a peak at $z \sim d/\theta$ (Fig. 1). Because of the finite outer scale, response to higher layers (more than $\sim$ 1 km, where $d_e > 10$m) falls off faster than $z^{-1/3}$. Hence a lunar scintillometer is a probe of the turbulence in the lower layers of the atmosphere. Diffraction effects are important when the relevant scales are less than the Fresnel radius $r_F = \sqrt{\lambda z}$. However, for lunar scintillations, $d_e \gg r_F$. Hence lunar scintillations are described by wavefront curvature alone (geometric optics) and are achromatic. Moreover, saturation is absent at these scales and so are the effects from the inner scale of turbulence.

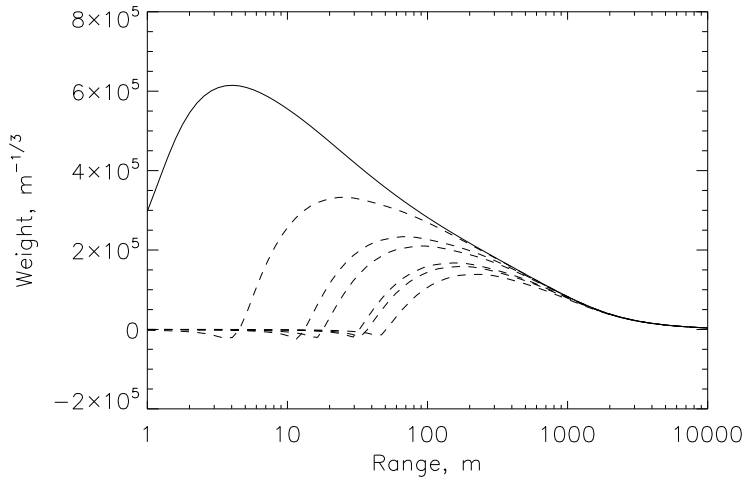

Figure 1. The weighting functions for all baselines for the current LuSci configuration. The single detector (zero baseline, diameter $\sim$ 1 cm) WF is shown in solid lines. The WFs for the finite baselines (dashed lines) show decreasing sensitivity to the lower altitudes with increasing baseline length (see Fig. 2 for the baseline lengths). The outer scale here is assumed to be 30 meters and is mainly responsible for the high-altitude fall-off of the response.

2. A SCINTILLOMETER ARRAY

An array of scintillometers can be used to reconstruct the seeing profile in the lower atmosphere as in the SHABAR instrument.[4] The normalized covariance ($C_I(r) = \frac{\langle \Delta I_1 \Delta I_2 \rangle}{\langle I_1 \rangle \langle I_2 \rangle}$) of the intensity fluctuations at two detectors separated at a (projected) "baseline" r is sensitive to turbulence at heights above that where the two "cones-of-sight" of the individual apertures overlap. This covariance is the Fourier transform of the 2D spatial power spectrum of the scintillation, which (for overhead measurement) is given by

$$W_I(f) \propto f^{-11/3} \lambda^{-2} \int_0^\infty C_n^2(h) G(f,h) sin(\pi \lambda h f^2)\, \mathrm{d}h \tag{3}$$

where G(f,h) represents the "windowing" function, a consequence of averaging the fluctuations as described above. From the above equation, it can be noted that the power spectrum has a nearly flat ($f^{-1/3}$) frequency dependence and hence the covariance (i.e. the Fourier transform) is almost proportional to the overlap integral of the averaging area.

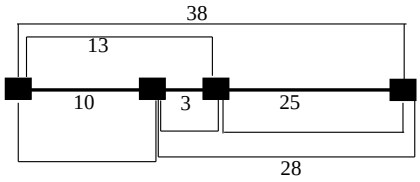

Figure 2. The current configuration of LuSci baselines, ranging from 3.5 to 38 cm

LuSci is a simple Lunar Scintillometer Array which aims to recover the GL turbulence profile. In its current configuration it consists of 4 photo diodes about a cm in diameter separated by "baselines" from 3.5 to 38 cm (Fig. 2). the covariance, $C_I(r)$, from a given pair of these detectors is given by

$$C_I(r) = \int_0^\infty W(r,z) C_n^2(z), \mathrm{d}z \tag{4}$$

where z is the distance along the line of sight and W is a *Weighting Function* (WF). The WF is the response of a baseline, r, to layers of unit turbulence integral J = $\int C_n^2 dh$ at different distances z (see Fig. 1). The WF is a function of the orientation of the baseline and the phase of the Moon. For our calculations, we model the Moon disk as an ellipse with effective diameter dependent on the Moon phase. The model is valid for the period from the first to the last quarter with a typical accuracy of 10% around the full Moon.

The prime goal of this work is to try and reconstruct the $C_n^2(h)$ profile from the covariance measurements with LuSci. First, we describe the instrument in the following section.

2.1 LuSci

LuSci is a linear array of photo diodes mounted on a simple box enclosure along the declination axis of an equatorial mounting. The mount is capable of tracking in RA, the wide field of view in the Dec axis obviating the need for tracking there. A minimal amount of baffling limits the FOV along the RA to $\sim$ 20 degrees. For a seeing of 1 arcsec at 500 nm wavelength, the turbulence integral J is 6.8×10^{-13} $m^{-1/3}$ (see Eqn. 1) and the WF is typically 2-3$\times10^5$, giving a scintillation index (normalized variance) of $\sim 4\times 10^{-8}$. To detect GL scintillation say a factor of 10 lower than this, the resolution of intensity measurement should be of the order of 3×10^{-5} which corresponds roughly to 16 bit digitization. LuSci uses Si photo diodes, operated on zero bias to eliminate dark current. The signal is amplified (2 stage) and digitized, before being recorded through a PC interface. The signal is sampled at 2 ms (with $\sim 10\times$ oversampling and averaging) and recorded in binary format in segments of a few seconds. Sky frames are recorded periodically. The covariances and dc values are recorded in ASCII format files, which also contain pointers to the corresponding segment of binary data. Fig. 3 is a schematic of the instrument.

The power spectrum of lunar scintillation recorded on a full Moon is shown in Fig. 4. The noise floor is of the order 1.5×10^{-11} Hz^{-1} and the instrument is basically photon-noise limited.

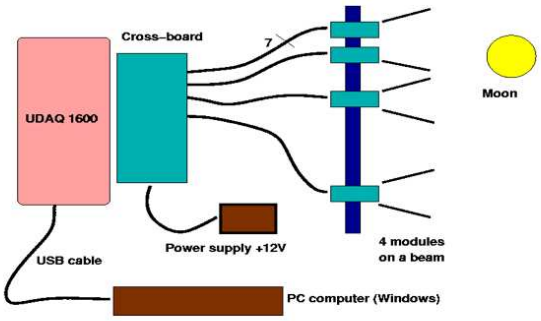

Figure 3. Schematic of LuSci showing the instrument set-up and data acquisition electronics

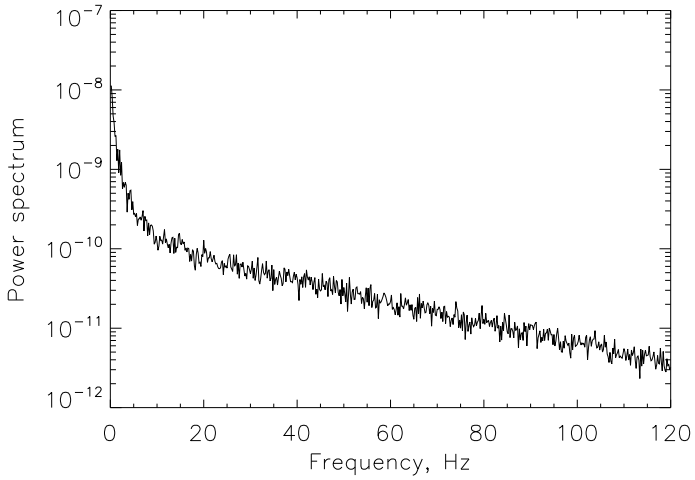

Figure 4. The DC-subtracted, normalized power spectrum recorded on the full Moon on Mar 18, 2008, at Penyon. The spectrum (units of Hz^{-1}) falls off steeply and approaches a noise floor beyond $\sim$ 150 Hz or so

3. RECONSTRUCTING THE TURBULENCE PROFILE

LuSci has now been deployed in several test campaigns on-site at CTIO (Cerro Tololo), the Las Campanas Observatory, ESO (Paranal) and the Penyon peak, the site for the upcoming Large Synoptic Survey Telescope (LSST). In this section we discuss the methods employed for profile reconstruction in the context of these campaigns. First, we wish to discuss the S/N ratios for the profile reconstruction. A full discussion is beyond the scope of this article, and we refer to Ref. 5. Briefly, the covariances measured by the different baselines are correlated to some degree. This is dominated by the slowly varying scintillation component originating in the high atmosphere. This statistical noise, not to be confused with instrument errors like detector noise, dominates the error budget even though our focus is the lower layers of the atmosphere. By calculating the error covariances, one can estimate the S/N of the reconstruction. Such an analysis for the specific 4-detector LuSci configuration (Fig. 2) discussed here leads to typical S/N for the reconstruction of 3-4 for a 20 s integration. Typically, in the following discussions, we use integration times of a minute to a few minutes per reconstruction point and the

S/N scales accordingly. We do not specifically discuss the errors hereafter.

3.1 The Layer Model

From the response functions shown in Fig. 1 for each baseline, it is evident that a weighted sum of these profiles can deliver an instrument response "shaped" to be sensitive to a fairly limited range of altitudes or "layer" in the atmosphere. This would be an intuitive method to exploit the natural response of the instrument to get a layer-by-layer reconstruction of the atmospheric turbulence.

A linear combination of the covariances in Eqn. 4 with some coefficients r_i would, in effect, sum the WFs with same weights to give a response

$$S(z_j) = \sum_{i=1}^{K} r_i W(z_j, b_i) \tag{5}$$

We aim for responses that would peak over a selected range of altitudes and be zero elsewhere, with overlapping ranges and ideally summing to unity. We use the matrix form and singular value decomposition to calculate the coefficients r as a matrix product of the weight matrix (dimension of baselines × altitude points) and desired response vector (length = number of altitude points).. The actual response, S, will of course differ from the ideal one, S_0. We minimise the difference in the least-squares sense to get the best possible solution.

$$\sum_{j=1}^{N} p_j [S(z_j) - S_0(z_j)]^2 = min \tag{6}$$

where N is the number of selected altitude points and p_j are a set of weights which emphasise the required altitudes for peak response. In practice, the baseline configuration of the instrument will decide the "favorable" altitudes for a smooth, well-defined response. We inspect the responses derived in the above fashion for all altitudes and choose the best set for the given detector configuration. A set of response functions with logarithmic FWHM of ~ 3 derived in this fashion are shown in Fig. 5.

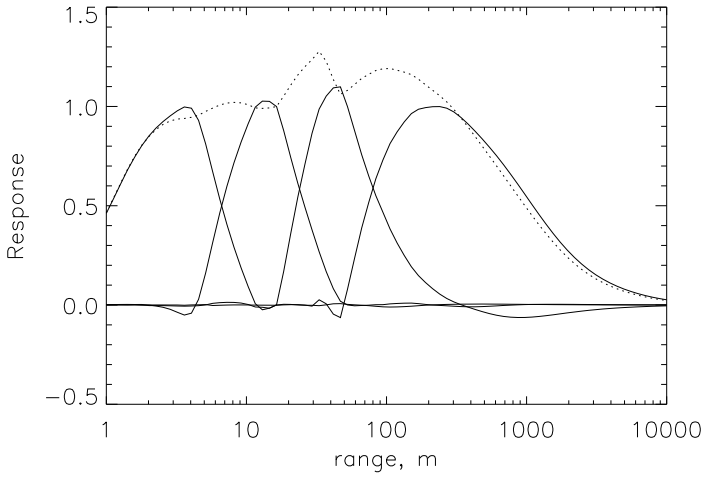

Figure 5. Response functions for all baselines for the "layer-profile" reconstruction.

LuSci was used at CTIO in February-March 2007 to gather data on or very close to the full Moon period. Fig. 6, Fig. 7 shows the "layer" restoration for a couple of nights from this campaign. The plot shows the seeing for a set of layers (cumulative sum up to each layer). We also show the simultaneous seeing measured by the MASS (Multi Aperture Scintillation Seeing) and DIMM (Differential Image Motion Monitor) instruments.[6] MASS measures the turbulence in the free (above the GL) atmsophere whereas DIMM measures the total seeing,

so the difference (the plotted quantity) is a good independent check for the GL seeing. The plots show good agreement between the LuSci measurements and DIMM-MASS seeing. Both nights have fairly good seeing, but the profile clearly shows that for the night of Feb 05, the seeing originates mostly in the high (200 m) layer, whereas for March 05, the lower (4, 16 m) layers contribute more. Subsequent data gathered over several nights at Campanas and Penyon have confirmed this method to be a robust restoration.

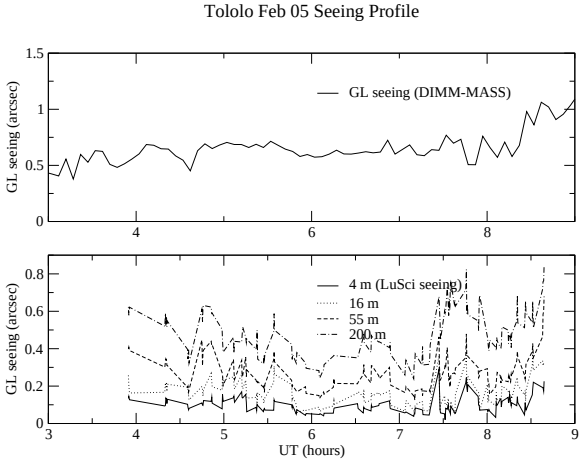

Figure 6. "Layer" reconstruction for the night of Feb 05, 2007, on Tololo. The layer model is not corrected for airmass.

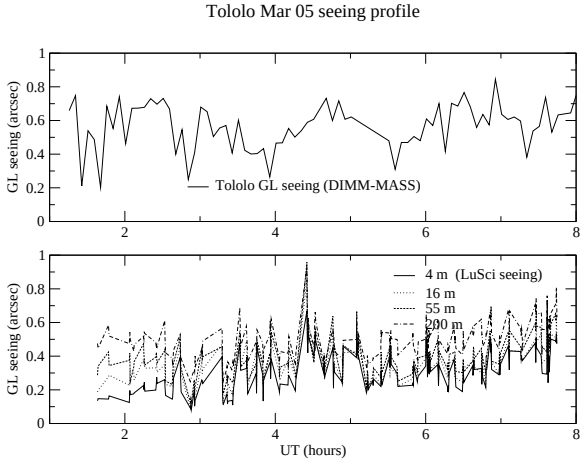

Figure 7. "Layer" reconstruction for the night of Mar 05, 2007, on Tololo. The layer model is not corrected for airmass.

3.2 Exponential Profile

While the layer model is a robust and intuitive restoration which is in fact not a formal "model" fitting, but a simple exploitation of the instrument's natural response, it suffers from relatively low altitude resolution ($\Delta z/z \sim 3-4$). Moreover, given the set instrument response to different ranges, it is difficult to correct for the airmass, i.e., vary the ranges to correct for the sec(z) factor. Besides, for most applications like site characterization for AO, a continuous profile is called for. Inspired by the exponential decay model adopted for the Cerro Pachon (site of the Gemini and SOAR telescopes) turbulence by Ref. 1, we try such a model for fitting LuSci data here. The profile is fitted as the sum of two exponentials,

$$C_I(r) = A\int_0^\infty W(z,r)\exp(-z/z_1)\mathrm{d}z + B\int_0^\infty W(z,r)\exp(-z/z_2)\mathrm{d}z \tag{7}$$

where A and B are constants and z_1 and z_2 are the exponential scale heights. The integrals are calculated for a grid of altitudes z and the constants A, B arrived at for each pair of grid points z_1, z_2 by solving the linear equation. The best fit is then calculated by least-squares over the entire grid. In Fig:8, we show the result of the exponential fitting model for one night of data from Penyon. For comparison we show the layer model as well. The scale height shows good agreement with the layer reconstruction.

4. THE WIND SPEEDS

The scintillation data have rich information on the temporal evolution of the turbulent layers. The 2 dimensional spectrum of scintillation from a single layer can be directly converted to a temporal spectrum if one were to assume the "frozen" turbulence Taylor model, with a characteristic frequency V/d_e, where V is the velocity of the layer. The temporal spectrum is then given by,

$$W_I(\nu) = 1/V\int_{-\infty}^{+\infty} W_I(\nu/V, f_y)\,\mathrm{d}f_y \tag{8}$$

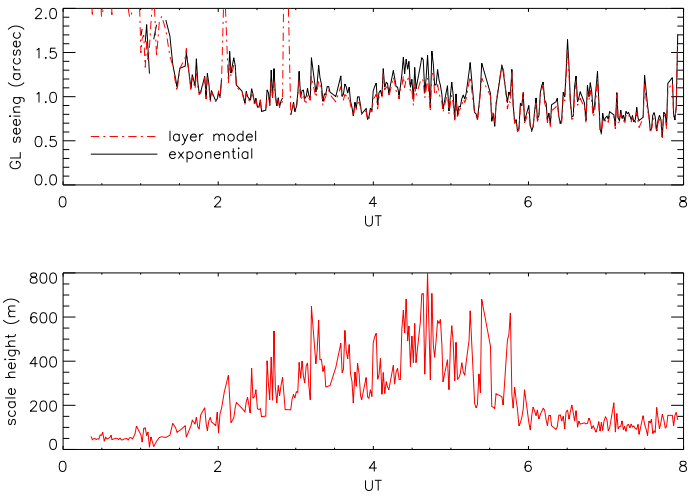

Figure 8. **Bottom**: The turbulence exponential scale height for the night of 23 March 2008, Penyon. The scale height shown is a weighted sum of z_1 and z_2 indicated in the text. Compare with the layer model in Fig. 9 **Top**: Comparison of total GL seeing between the exponential and layer reconstructions for the same night.

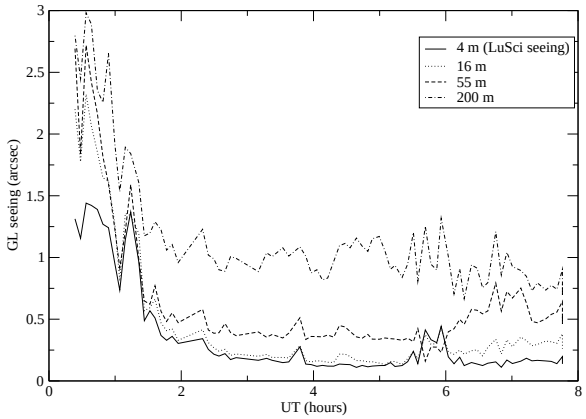

Figure 9. The layer profile reconstruction for March 23, 2008, Penyon. Compare with Fig. 8, the exponential decay model.

where W_I is as in Eqn. 3. The shift of the maximum of the temporal cross-correlation between the individual detector data is of course directly related to the wind speed if the Taylor hypothesis holds. However, recovering the wind profile from this is complicated by the fact that we have a linear array in one dimension and therefore no information about the orthogonal component of the wind vector. Moreover, the asymmetries induced by the phase and illumination pattern of the Moon and its projected angle to the array further worsen the situation. Here we try to reconstruct the wind profile using the temporal spectrum from a single detector. We reconstruct the location of the turbulence through the layer model. We then assume that the layers move according to a simple wind model

$$V = V_0 + \alpha z \tag{9}$$

where V_0 is the velocity on the ground and α is a gradient with altitude. The theoretical temporal spectrum in Eqn. 8 is modeled by a simple analytic expression (Fig. 10) with a coefficient (function of θ - the angular

diamter of the Moon, z - the range to the layer and d - the detector diameter) times a trigonometric function of the characteristic frequency, and we fit for the parameters V_0 and α, assuming that the spectrum arises as the sum of the contributions from the different layers. To justify the 2D symmetry, we limit ourselves to data taken during the full Moon and neglect any asymmetries in the Moon image.

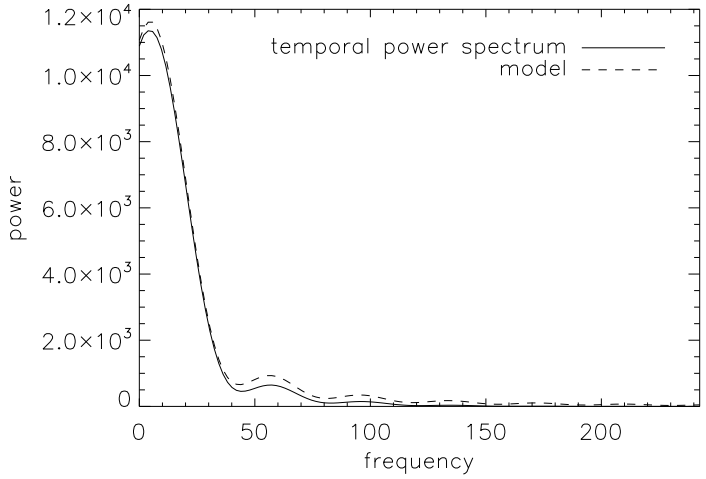

Figure 10. The analytical fit to the temporal spectrum for a layer moving at 10 ms^{-1} at 30 m altitude. The spectrum is in units of $m^{1/3}s$. The squared residual is $\sim 3\%$

We tested this wind-reconstruction during the 2008 Penyon campaign. A weather tower located near LuSci independently measured the wind profile at altitudes of 5, 12, 20 and 30 m, providing an excellent cross-calibration of our technique. We plot in Fig. 11, the reconstruction for the night of March 18 on Penyon. The weather tower recorded nearly identical velocities for the various heights, indicating that the slope was close to zero. We show the reconstructed ground-level velocity V_0 and also plot the wind velocity as recorded at the 5 m sensor. We have limited ourselves to those samples which provide good-to- moderate quality fits, with $\chi^2 \leq 10$. The wavefront projects on to the horizontal wind vector and so a $\sec(z)$ correction has been applied. The reconstruction is fairly successful in reproducing the overall trends in velocity and the results are encouraging.

5. SUMMARY

Lunar scintillations offer a robust and effective way of measuring GL turbulence. We have built and successfully tested LuSci, a scintillometer array, to yield the turbulence profile of the lower atmosphere. The scintillation method offers the advantages of achromaticity and is free of saturation and inner-scale effects. However, the signal is comparatively weak and the method is limited to a period around the full Moon (50% time coverage). We demonstrate a couple of different algorithms for turbulence profile reconstruction and a method to acquire the wind profile from LuSci data. The layer-model is robust, but has limitations in not yielding a continuous profile and being difficult to correct for airmass effects. In the near future, we will develop a continuous profile reconstruction method. LuSci is being completely automated, with improved mounting, and a full cross-calibration campaign will be undertaken over the next few months to take the instrument to maturity.

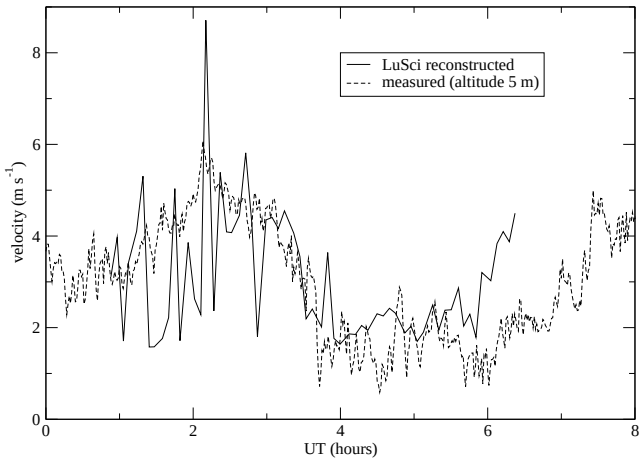

Figure 11. The measured wind velocity on March 18, 2008, Penyon, at the 5 m sensor compared to the reconstructed wind velocity at ground level. The general trend is similar to the measured velocity. The reconstructed slope (not shown) is close to zero, which is validated by the tower measurement as well.

REFERENCES

[1] Tokovinin, A., & Travouillon, T. 2006, *MNRAS*, 365, 1235
[2] Roddier, F. 1981, Prog. Optics, Volume 19, p. 281-376, 19, 281
[3] Tatarski, V.I. 1961, *Wave Propogation in Turbulent Medium*
New York: McGraw-Hill
[4] Beckers, J.M. 2001, *Experimental Astronomy*, 12, 1
[5] Tokovinin 2008. Unpublished technical note:
Random measurement errors in LuSci. February 12, 2008
http://www.ctio.noao.edu/ atokovin/profiler/errcalc.pdf
[6] Tokovinin, A., & Kornilov, V. 2007, *MNRAS*, 381, 1179